Published in final edited form as:
AJR Am J Roentgenol. 2009 March ; 192(3): W84–W89. doi:10.2214/AJR.08.1381.

Coronary Plaque Quantification by Voxel Analysis: Dual-Source MDCT Angiography Versus Intravascular Sonography

Harald Brodoefel[1,2], **Christof Burgstahler**[3], **Adeel Sabir**[1], **Chun-Shan Yam**[1], **Faisal Khosa**[1], **Claus D. Claussen**[2], and **Melvin E. Clouse**[1]

[1]Department of Radiology, Beth Israel Deaconess Medical Center, Harvard Medical School, 330 Brookline Ave., WCC-302, Boston, MA 02215

[2]Department of Diagnostic Radiology, Eberhard-Karls-University, Tübingen, Germany

[3]Department of Cardiology, Eberhard-Karls-University, Tübingen, Germany

Abstract

OBJECTIVE—The purpose of this study was to evaluate a voxel-based analytic technique for quantification of noncalcified coronary artery plaque with intravascular sonography as a standard of reference.

SUBJECTS AND METHODS—Intravascular sonography and dual-source MDCT angiography prospectively performed on 12 patients resulted in identification of 20 segments containing noncalcified plaque. Four of these segments were used to establish reference measurements of 0.6-mm proximal wall thickness with a 0-HU cutoff between the epicardial fat and outer wall and an individually adjusted threshold for the interface between the wall and lumen. With these data, consecutive circular layers of the outer wall were subtracted from a 3D volume to determine the plaque plus medial layer and the actual plaque volume in the other 16 segments. Accuracy of the voxel technique was assessed by comparing the results with intravascular sonographic findings.

RESULTS—Both the total plaque burden (plaque plus medial layer) and the actual plaque volume had good concordance with intravascular sonographic findings (49.6 ± 20 mm^3 vs 56.7 ± 23.6 mm^3, $p = 0.076$; 26.5 ± 14.8 mm^3 vs 30.9 ± 15.3 mm^3, $p = 0.09$). Corresponding correlation coefficients were $r = 0.76$ and $r = 0.79$. The method had good reproducibility, the an intraclass correlation coefficients being 0.93 for total plaque burden and 0.90 for actual plaque volume.

CONCLUSION—Voxel analysis can be used for accurate and reproducible quantification not only of plaque burden but also of actual plaque volume.

Keywords

dual-source CT; intravascular sonography; MDCT angiography; plaque burden; voxel analysis

Vulnerable and often nonobstructive plaque is acknowledged as the primary cause of acute coronary syndrome [1–3]. Therefore, accurate quantification of individual plaque burden is important for risk stratification and monitoring of lipid-lowering therapy [4, 5]. Invasive coronary angiography is the accepted reference standard for detection of intraluminal and obstructive atheroma. However, because of the phenomenon of vessel remodeling,

Address correspondence to M. E. Clouse (mclouse@bidmc.harvard.edu).

WEB
This is a Web exclusive article.

nonobstructive plaque may be missed with invasive coronary angiography until the late stage of the disease [6–8]. Because of its spatial resolution, intravascular sonography has unprecedented accuracy in plaque detection and quantification [9–11], yet the method is limited to proximal vessel segments, is expensive, and is associated with considerable procedural risks.

MDCT has gained widespread acceptance as a noninvasive alternative to coronary angiography in selected patients [12]. Although MDCT angiography (MDCTA) has repeatedly proved its potential for detection and classification of intraluminal and extraluminal atheroma, its ability to accurately depict plaque burden is restricted by insufficient reproducibility [13–19]. In addition to fundamental limitations such as spatial and temporal resolution of scanners, the principal cause of high interobserver variability has been the need for manual segmentation of the boundaries of lumen, vessel, and plaque [14]. To overcome this problem, we developed a semiautomated algorithm based on gradient change in attenuation plotted across the vessel, segmenting the arterial wall and lumen to arrive at a volumetric measurement of noncalcified plaque. In the initial phase of a pilot study, this approach had high reproducibility of plaque quantification [20, 21]. However, precision of volumetric measurements was not evaluated in a head-to-head comparison with findings at intravascular sonography. The aim of this feasibility study was to assess the accuracy of advanced dual-source MDCTA and voxel analysis in determining the volume of noncalcified plaque with intravascular sonography as the standard of reference.

Subjects and Methods

Study Population

From September 2006 to May 2007 we conducted a study with 100 patients (mean age, 64 ± 9 [SD] years; 73 men) scheduled for conventional coronary angiography because of suspected coronary artery disease or suspected progression of known coronary artery disease. All dual-source CT studies were performed the day before conventional angiography. The study was approved by the institutional review board, and all subjects provided written informed consent. Exclusion criteria were renal insufficiency (serum creatinine concentration > 1.5 mg/dL), hyperthyroidism (basal concentration of thyroid-stimulating hormone < 0.03 μL/L in combination with elevated thyroid hormone levels in the peripheral blood), known allergic reaction to iodinated contrast media, and inability to perform a breath-hold as instructed. The patients were instructed not to consume caffeine after 12 midnight.

Twelve of the patients (11 men, one woman; mean age, 65 ± 7 years) underwent intravascular sonography of at least one vessel as part of the catheterization procedure for evaluation of coronary vessels without angiographic evidence of stenosis of greater than 50% reduction in vessel diameter. In these 12 patients, 20 atherosclerotic lesions were chosen for further analysis. Selection criteria for lesions were absence of macroscopic calcification on CT angiography and presence of suitable fiducial markers of unequivocal identification.

Dual-Source MDCTA: Imaging

All studies were performed with a dual-source CT scanner (Somatom Definition, Siemens Medical Solutions). Before acquisition of the topogram, patients received a single dose of 0.8 mg glycerol trinitrate. For contrast-enhanced scans, vessel opacification was achieved with automated injection through a power injector (CT2TM, Medtron) of 80 mL iomeprol (Iomeron 400, Bracco) at a flow rate of 5 mL/s plus a 60-mL chaser bolus. Estimation of individual circulation times was based on the test bolus technique with a 20-mL bolus and

dynamic evaluation software (DynEva, Siemens Medical Solutions). Collimation was 32 × 0.6 mm; slice acquisition, 64 × 0.6 mm with the *z*-flying focal spot technique; gantry rotation time, 330 milliseconds; pitch, 0.20–0.43 adapted to heart rate; tube voltage, 120 kV; and maximum tube current, 400 mAs per rotation. For dose reduction, prospective tube current modulation was applied: For heart rates less than 60 beats/min, full tube current was applied from 60% to 70% of the cardiac cycle; at 60–70 beats/min, from 50% to 80%; and at heart rates greater than 70 beats/min, from 30% to 80% of the cardiac cycle.

An initial reconstruction window was based on the results of a test series of images obtained in the transverse plane at the level of segment 2 that displayed reconstruction window offsets by 5% of the entire cardiac cycle. If motion artifacts were present in the initial reconstruction, further reconstructions were obtained in 5% increments of the cardiac cycle until all individual arteries were visualized at optimal image quality.

In all patients, a single-segment reconstruction algorithm was used that resulted in a temporal resolution of 83 milliseconds. Reconstruction parameters included a 170 × 170 mm field-of-view, 512 × 512 matrix, medium soft convolution kernel (B26f), effective slice thickness of 0.75 mm, and a reconstruction increment of 0.4 mm.

Dual-Source MDCTA: Data Analysis

Plaque burden was evaluated by voxel analysis with Analyze 7 software (Analyze Direct) in a standalone PC-based workstation. In this attenuation-based analysis approach, thresholds were used to segment arterial wall and plaque. Optimal thresholds were normalized for every patient or segment by plotting of radial lines across epicardial fat, normal arterial wall, and lumen. An attenuation value of 0 HU was defined as a reference point for the interface between epicardial fat and the outer arterial wall. Evaluation of plaque was performed according to the following two-step protocol.

Step 1: Arterial wall calibration—The purpose of the first step was to determine the arterial wall thickness to use in the voxel analysis. This step was performed by an experienced radiologist (reader 1) not blinded to the intravascular sonographic results. Four plaques in four patients were studied to calibrate the voxel analysis technique to intravascular sonography. One of these lesions was located in the left main coronary artery, two in the proximal left anterior descending coronary artery, and one in the proximal right coronary artery. Mean vessel diameter in the calibration cohort was 5.6 ± 0.3 mm (range, 5.4–6.1 mm). Accurate matching of corresponding lesions was ensured by referring to lesion length and fiducial markers (stents, side branches, and characteristic calcifications) defined with longitudinally reconstructed intravascular sonographic data. A maximal measurement discrepancy of 5% was accepted with regard to length of segment.

To determine the average thickness of the normal arterial wall, three radial lines were plotted across the arterial wall of the normal adjacent segments, notably from the epicardial fat to the center of the lumen. Attenuation values of consecutive isotropic 200-μm voxels were obtained from the outside arterial wall into the lumen. The first voxel with a positive attenuation value was defined as being the first within the vessel wall. According to recent literature [20, 22–25] on the attenuation cutoffs between arterial wall and lumen, a voxel with an attenuation value greater than 160 HU was defined as being the first voxel within the lumen. On the basis of this assumption, the average wall thickness in our calibration cohort was determined to be three 200-μm voxels (0.6 mm). In both the calibration and the analysis series, the threshold between wall and lumen was thus defined with the following formula: (attenuation of third positive voxel + attenuation of fourth positive voxel)/2.

With the threshold for the outer wall boundary set to 0 HU, the software generated a 3D volume of the entire arterial segment and then successively removed the wall-containing voxels from the outside to the inside of the vessel. At the same time, voxels with attenuation values characteristic of the lumen were subtracted. Comparing the volumetric results to findings at intravascular sonography, we found that removal of only one outer wall voxel resulted in a volume equivalent to the entire plaque burden (51.6 ± 5.9 vs 47.8 ± 8.6 mm^3). Removal of another voxel resulted in a volume that matched the pure plaque volume without the medial layer (22.6 ± 5.4 vs 17.5 ± 2.6 mm^3).

Step 2: Plaque analysis—Analysis of another 16 plaque-containing segments (distributed in eight patients) was performed by reader 1, who for this step was blinded to the corresponding intravascular sonographic findings. Matching of corresponding lesions was ensured by both lesion length and fiducial markers. A maximal measurement discrepancy of 5% was accepted with regard to the length of the target lesion. For all lesions, the attenuation cutoff between wall and lumen was determined in an adjacent normal vessel segment. Three radial lines were plotted across the epicardial fat, wall, and lumen, and thresholds were calculated as in step 1. By subtraction of first one and then two of the outer-wall voxels, atheroma was finally quantified in terms of plaque plus medial layer or actual plaque volume. The average time needed to perform step 2 was 15 minutes.

Standardized 0.02-cm^2 region of interest measurements were used in the plaque-containing segments to determine the maximal attenuation in the lumen (mean of three measurements). The first SD of CT attenuation within the regions of interest was assessed and defined as image noise level. For evaluation of interobserver variability in the assessment of plaque volume, step 2 was repeated by a blinded reader 2. For assessment of intraobserver variability, plaque measurements were repeated by reader 1 after a 6-month interval.

Intravascular Sonography: Imaging

Intravascular sonographic and intravascular sonographic–virtual histologic data were acquired with a dedicated console. A phased-array 20-MHz 3.2-French intravascular sonographic catheter (Eagle Eye, Volcano) was placed in a position distal to the lesion of interest. Motorized pullback was performed at a pullback rate of 0.5 mm/s. The pullback was stopped as soon as the intravascular sonographic catheter reached the guiding catheter. During pullback, a gray-scale intravascular sonogram was recorded, and raw radiofrequency data were captured at the top of the R wave.

Intravascular Sonography: Data Analysis

Intravascular sonographic–virtual histologic data were transferred to an offline workstation and reconstructed with a commercial software tool (pcVH 2.1 software, Volcano). Studies were evaluated by a single experienced observer blinded to the results of dual-source MDCTA. The lumen and the medial–adventitial interface were defined by semiautomatic contour detection. Maximal vessel diameter of the plaque-containing segment was assessed. Further morphometric parameters were expressed as cross-sectional area for every frame. Area of total plaque burden was defined as plaque plus medial layer and calculated as vessel area minus lumen area. The software also was used to calculate the volume of various plaque components. The latter summed to the actual plaque volume, which corresponded to plaque burden minus the volume of the medial layer.

Statistical Analysis

Bland-Altman analysis was used to display the systematic error and CI between measurements. Correlation between CT and intravascular sonographic variables was assessed in terms of Pearson’s correlation coefficient. Pearson’s correlation also was used to

quantify the association between attenuation cutoffs and maximal luminal attenuation. Interobserver reliability was assessed by calculation of the two-way random single-measure intraclass correlation coefficient. Intra-observer reliability was assessed with one-way random intraclass correlation coefficient. In addition, interobserver and intraobserver variability were expressed as percentages and calculated with the following formula [14]: (volume observer 1 − volume observer 2)/[(0.5 × volume observer 1) + (0.5 × volume observer 2)]. All variables were expressed as mean ± SD. Comparisons of plaque volumes were performed with the Student's *t* test for paired observations. A value of $p < 0.05$ indicated statistical significance. Statistical calculations were performed with commercially available software (JMP version 6, SAS Institute; Prism version 4.00, GraphPad; SPSS version 15, SPSS).

Results

In the analysis cohort, the distributions of lesions and average vessel diameters were as follows: three lesions in the left main coronary artery (6.1 ± 0.1 mm); five lesions in the left anterior descending coronary artery (four in segment 6; one in segment 7; 5.4 ± 0.4 mm), five lesions in the circumflex coronary artery, all in segment 11 (5.4 ± 0.4 mm), and three lesions in the right coronary artery (two in segment 1; one in segment 2; 5.5 ± 0.3 mm). In all patients, plaque-containing segments were unequivocally identified through fiducial markers and segment length.

Dual-source CT showed a mean total plaque burden of 49.6 ± 20 mm^3 and actual plaque volume of 26.5 ± 14.8 mm^3. Intravascular sonography showed a mean total plaque burden of 56.7 ± 23.6 mm^3 and an actual plaque volume 30.9 ± 15.3 mm^3. According to Bland-Altman analysis, there was good concordance between techniques for volumetric measurements (Fig. 1). The trend toward underestimation of total plaque burden and overestimation of actual plaque volume ($p = 0.076$) was not significant ($p = 0.09$). The correlation coefficients were $r = 0.76$ for total plaque burden and $r = 0.79$ for actual plaque volume (Fig. 2).

Intraclass correlation coefficients for interobserver assessment were 0.93 for total plaque burden and 0.90 for actual plaque volume. The intraclass coefficients for intraobserver assessment were 0.94 and 0.92. The corresponding percentage interobserver variability rates were 13% and 17% and the intraobserver variability rates, 13% and 15%.

In the analysis cohort, the mean optimal attenuation cutoff between inner wall and lumen was 164 ± 14 HU. The mean maximal luminal attenuation in the analyzed segments was 419 ± 67 HU (range, 290–504 HU). The average corresponding SD was 19.3 ± 7 HU (range, 11–34 HU). There was significant correlation between CT attenuation in the plaque-containing segment of lumen and the individually normalized attenuation cutoff for the wall–lumen interface ($r = 0.64$, $p = 0.003$). In contrast, image noise level did not correlate with the optimal attenuation threshold for lumen ($r = 0.1$, $p = 0.88$). Imaging examples are provided in Figures 3 and 4.

Discussion

Our primary finding is that voxel analysis with successive subtraction of outside wall layers may adequately and reproducibly quantify not only the entire plaque burden (plaque plus medial layer) but also the actual volume of noncalcified plaque. Regarding plaque burden in our study, the degree of correlation with intravascular sonographic findings is in line with results of previous investigations by Achenbach et al. [13] and Leber et al. [14], who found coefficients of variation of 0.80 and 0.69, respectively. Notably, in both series, plaque was manually segmented. In a more recent study by Sun et al. [25], who also used automated

attenuation-based analysis for plaque quantification, the correlation with intravascular sonography was $r = 0.77$. Although these data do not suggest an obvious advantage of voxel analysis in terms of plaque quantification, the reproducibility of volumes improves considerably when an attenuation-based approach is used [25].

Interobserver variability in our collective was 0.93 (intraclass correlation coefficient), or 13%, for plaque plus medial layer, and 0.90 (intraclass correlation coefficient), or 17%, for actual plaque volume; likewise, it was as low as 12% in the study by Sun et al. [25]. A major cause of reduced variability is that manual adjustments for luminal and outer wall boundaries are not required for voxel analysis. Moreover, results do not depend on subjective choice of window level and width. With manual segmentation of plaque, interobserver variability has been reported to be as high as 37% [14].

A primary characteristic of our method is that the interface between epicardial fat and outer wall is used as a reference point and consecutive circular layers of the wall are removed to arrive at the plaque plus medial layer or the actual plaque volume. In our study, subtraction of a one-voxel (0.2 mm) layer resulted in a volume that matched the plaque plus medial layer at intravascular sonography but with a tendency toward underestimation at dual-source MDCTA. This circular layer corresponds to the adventitial component, which is readily visualized at cross-sectional imaging. Another one-voxel subtraction proved equivalent to removal of the medial layer at intravascular sonography, even though this subtraction showed a trend toward overestimation of the intravascular sonographic volume.

Ultimately, our technique of subtracting the medial layer is analogous to that by which the intravascular sonographic software determines the volume of the actual plaque tissue. Because neither gray-scale nor radiofrequency analysis in intravascular sonography–virtual histology may adequately differentiate plaque tissue from medial layer, in the computer program, an assumption is made about the thickness of the medial layer in terms of a subtractable circular volume [26, 27].

A further asset to the voxel histogram technique is calculation of optimal thresholds for vessel lumen in every patient and arterial segment. Because of partial volume effects, the magnitude of luminal enhancement exerts a considerable influence on the attenuation of adjacent structures, such as the inner wall and plaque. This phenomenon was found in an investigation of plaque quantification by attenuation-based analysis [25]. Likewise, in our study, there was a significant association between the optimal cutoff for luminal and maximal luminal attenuation. We speculate that individual adjustment of the respective threshold may contribute to the consistency of measurement in the scenario of variable luminal contrast enhancement between and within patients.

Calculation of thresholds for vessel lumen was based on findings from our initial calibration experiment; a three-voxel (0.6 mm) thickness was assumed for normal proximal arterial wall. Compared with the MRI measurement (0.75 mm) and results from previous CT studies on the voxel analysis technique (0.8 mm), thickness of normal wall was found to be slightly smaller in our analysis [20, 28]. This discrepancy is best explained by our use of a comparatively high 2 g/s iodine delivery rate. The latter leads to improved, 419-HU CT attenuation in the vessel lumen and results in smaller measurements of wall thickness owing to partial volume effects on the wall–lumen interface. In one study [20], the much lower iodine delivery rate of 1.4 g/s was used. Accordingly, mean CT attenuation was only 315 HU, resulting in a 0.8-mm assumption for proximal normal wall. These observations suggest that initial calibration steps should be performed whenever changes in contrast or scan protocols suggest a major effect on vessel attenuation.

We acknowledge the following limitations of this feasibility study. First, the number of observations was small, and results will have to be confirmed in larger series. Volumes of total plaque burden and actual plaque were compared by means of intravascular sonography–virtual histology. Because this report is the first, to our knowledge, on CT-based segmentation of actual plaque volume, results will have to be confirmed in future correlations with histologic findings.

Because intravascular sonography can be performed only in proximal segments, plaque in the distal coronary arteries was not evaluated in our study. In far distal segments our technique has to be adjusted for decreased vessel wall thickness. The emphasis of the voxel analysis technique is on quantification of noncalcified plaque. Owing to CT attenuation values beyond those of intraluminal contrast enhancement, calcified plaques or plaque components cannot be assessed with our approach. Likewise, classification of atheroma in terms of plaque composition was not addressed.

The reproducibility of volume measurements has been assessed only in terms of interobserver and intraobserver agreement. The robustness of the method in serial follow-up and the scenario of variable intraluminal contrast enhancement needs to be proved in further investigations, such as animal studies. Finally, attenuation thresholds as used in our study depend partly on distinct imaging parameters and reprojection filters. With use of variable reconstruction techniques, results may be different, and individual calibration is mandatory.

We conclude that our results with voxel analysis technique suggest the potential for adequate and reproducible quantification of noncalcified atheroma in terms of both total plaque burden and volume of the actual plaque tissue. Whether quantification of actual plaque is advantageous in the assessment of serial plaque stabilization remains open to further investigation. Our approach should be compared with the use of commercial attenuation-based analysis software programs for determining the best algorithm for accurate MDCTA quantification of plaque.

Acknowledgments

Funded by National Institutes of Health grant NHLBI P50-HL-083813.

References

1. Falk E. Pathogenesis of atherosclerosis. J Am Coll Cardiol. 2006; 47:C7–C12. [PubMed: 16631513]
2. Fuster V, Badimon L, Badimon JJ, Chesebro JH. The pathogenesis of coronary artery disease and the acute coronary syndromes (2). N Engl J Med. 1992; 326:310–318. [PubMed: 1728735]
3. Ross R. The pathogenesis of atherosclerosis: a perspective for the 1990s. Nature. 1993; 362:801–809. [PubMed: 8479518]
4. Fayad ZA, Fuster V, Nikolaou K, Becker C. Computed tomography and magnetic resonance imaging for noninvasive coronary angiography and plaque imaging: current and potential future concepts. Circulation. 2002; 106:2026–2034. [PubMed: 12370230]
5. Taylor AJ, Merz CN, Udelson JE. 34th Bethesda Conference: executive summary—can atherosclerosis imaging techniques improve the detection of patients at risk for ischemic heart disease? J Am Coll Cardiol. 2003; 41:1860–1862. [PubMed: 12798552]
6. Mintz GS, Painter JA, Pichard AD, et al. Atherosclerosis in angiographically “normal” coronary artery reference segments: an intravascular ultrasound study with clinical correlations. J Am Coll Cardiol. 1995; 25:1479–1485. [PubMed: 7759694]
7. Nissen SE, Gurley JC, Grines CL, et al. Intravascular ultrasound assessment of lumen size and wall morphology in normal subjects and patients with coronary artery disease. Circulation. 1991; 84:1087–1099. [PubMed: 1884441]

8. Topol EJ, Nissen SE. Our preoccupation with coronary luminology: the dissociation between clinical and angiographic findings in ischemic heart disease. Circulation. 1995; 92:2333–2342. [PubMed: 7554219]
9. Nishimura RA, Edwards WD, Warnes CA, et al. Intravascular ultrasound imaging: in vitro validation and pathologic correlation. J Am Coll Cardiol. 1990; 16:145–154. [PubMed: 2193046]
10. Potkin BN, Bartorelli AL, Gessert JM, et al. Coronary artery imaging with intravascular high-frequency ultrasound. Circulation. 1990; 81:1575–1585. [PubMed: 2184946]
11. Yock PG, Linker DT. Intravascular ultrasound: looking below the surface of vascular disease. Circulation. 1990; 81:1715–1718. [PubMed: 2184950]
12. Schroeder S, Achenbach S, Bengel F, et al. Cardiac computed tomography: indications, applications, limitations, and training requirements—report of a writing group deployed by the Working Group Nuclear Cardiology and Cardiac CT of the European Society of Cardiology and the European Council of Nuclear Cardiology. Eur Heart J. 2008; 29:531–556. [PubMed: 18084017]
13. Achenbach S, Moselewski F, Ropers D, et al. Detection of calcified and noncalcified coronary atherosclerotic plaque by contrast-enhanced, sub-millimeter multidetector spiral computed tomography: a segment-based comparison with intravascular ultrasound. Circulation. 2004; 109:14–17. [PubMed: 14691045]
14. Leber AW, Becker A, Knez A, et al. Accuracy of 64-slice computed tomography to classify and quantify plaque volumes in the proximal coronary system: a comparative study using intravascular ultrasound. J Am Coll Cardiol. 2006; 47:672–677. [PubMed: 16458154]
15. Leber AW, Knez A, Becker A, et al. Accuracy of multidetector spiral computed tomography in identifying and differentiating the composition of coronary atherosclerotic plaques: a comparative study with intracoronary ultrasound. J Am Coll Cardiol. 2004; 43:1241–1247. [PubMed: 15063437]
16. Leber AW, Knez A, von Ziegler F, et al. Quantification of obstructive and nonobstructive coronary lesions by 64-slice computed tomography: a comparative study with quantitative coronary angiography and intravascular ultrasound. J Am Coll Cardiol. 2005; 46:147–154. [PubMed: 15992649]
17. Moselewski F, Ropers D, Pohle K, et al. Comparison of measurement of cross-sectional coronary atherosclerotic plaque and vessel areas by 16-slice multidetector computed tomography versus intravascular ultrasound. Am J Cardiol. 2004; 94:1294–1297. [PubMed: 15541250]
18. Schoenhagen P, Tuzcu EM, Stillman AE, et al. Non-invasive assessment of plaque morphology and remodeling in mildly stenotic coronary segments: comparison of 16-slice computed tomography and intravascular ultrasound. Coron Artery Dis. 2003; 14:459–462. [PubMed: 12966267]
19. Schroeder S, Kopp AF, Baumbach A, et al. Noninvasive detection and evaluation of atherosclerotic coronary plaques with multislice computed tomography. J Am Coll Cardiol. 2001; 37:1430–1435. [PubMed: 11300457]
20. Clouse ME, Sabir A, Yam CS, et al. Measuring noncalcified coronary atherosclerotic plaque using voxel analysis with MDCT angiography: a pilot clinical study. AJR. 2008:190. [web]1553–1560. [PubMed: 18562745]
21. Sabir A, Yam CS, Yoshimura N, et al. Measuring noncalcified coronary atherosclerotic plaque using voxel analysis with MDCT angiography: phantom validation. AJR. 2008; 190:947. [Web] W242–W246.
22. Carrascosa PM, Capunay CM, Garcia-Merletti P, Carrascosa J, Garcia MF. Characterization of coronary atherosclerotic plaques by multidetector computed tomography. Am J Cardiol. 2006; 97:598–602. [PubMed: 16490420]
23. Iriart X, Brunot S, Coste P, et al. Early characterization of atherosclerotic coronary plaques with multidetector computed tomography in patients with acute coronary syndrome: a comparative study with intravascular ultrasound. Eur Radiol. 2007; 17:2581–2588. [PubMed: 17549491]
24. Pohle K, Achenbach S, Macneill B, et al. Characterization of non-calcified coronary atherosclerotic plaque by multi-detector row CT: comparison to IVUS. Atherosclerosis. 2007; 190:174–180. [PubMed: 16494883]

25. Sun J, Zhang Z, Lu B, et al. Identification and quantification of coronary atherosclerotic plaques: a comparison of 64-MDCT and intravascular ultrasound. AJR. 2008; 190:748–754. [PubMed: 18287448]

26. Nair A, Kuban BD, Tuzcu EM, Schoenhagen P, Nissen SE, Vince DG. Coronary plaque classification with intravascular ultrasound radiofrequency data analysis. Circulation. 2002; 106:2200–2206. [PubMed: 12390948]

27. Nair A, Margolis P, Kuban BD, Vince DG. Automated coronary plaque characterisation with intravascular ultrasound backscatter: ex vivo validation. EuroIntervention. 2007; 3:113–120. [PubMed: 19737694]

28. Fayad ZA, Fuster V, Fallon JT, et al. Noninvasive in vivo human coronary artery lumen and wall imaging using black-blood magnetic resonance imaging. Circulation. 2000; 102:506–510. [PubMed: 10920061]

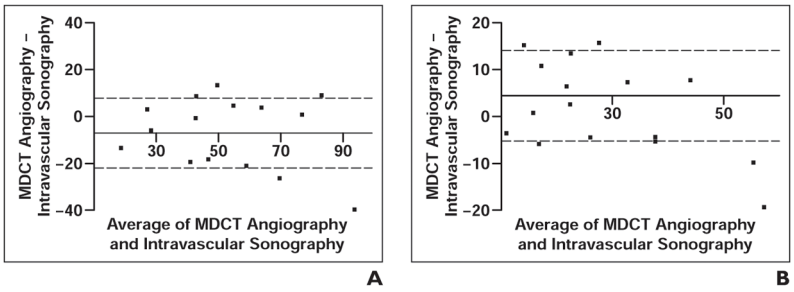

Fig. 1. Concordance between MDCT angiography and intravascular sonography in depiction of plaque

A and **B,** Bland-Altman plots show total plaque burden (**A**) and actual plaque volume (**B**) as obtained with MDCT angiography and intravascular sonography. Point of intersection between *x*- and *y*-axes indicates bias of MDCT angiography. Dotted lines indicate 1 SD of bias.

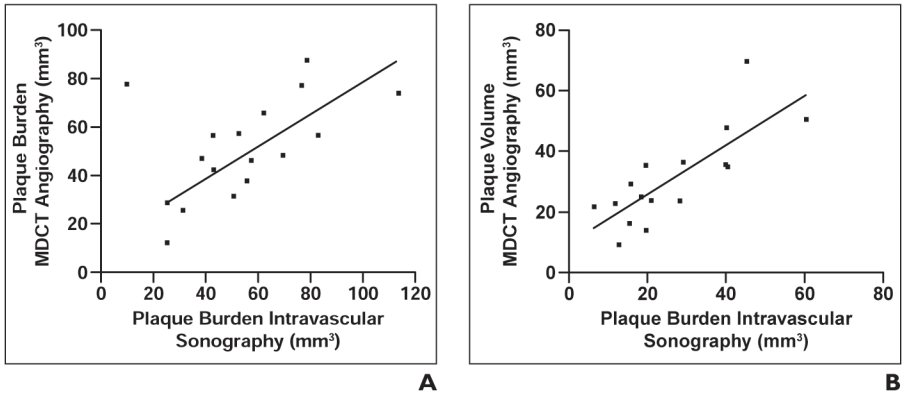

Fig. 2. Correlation between MDCT angiography and intravascular sonography in depiction of plaque

A and **B,** Graphs show correlation of total plaque burden (**A**) and actual plaque volume (**B**).

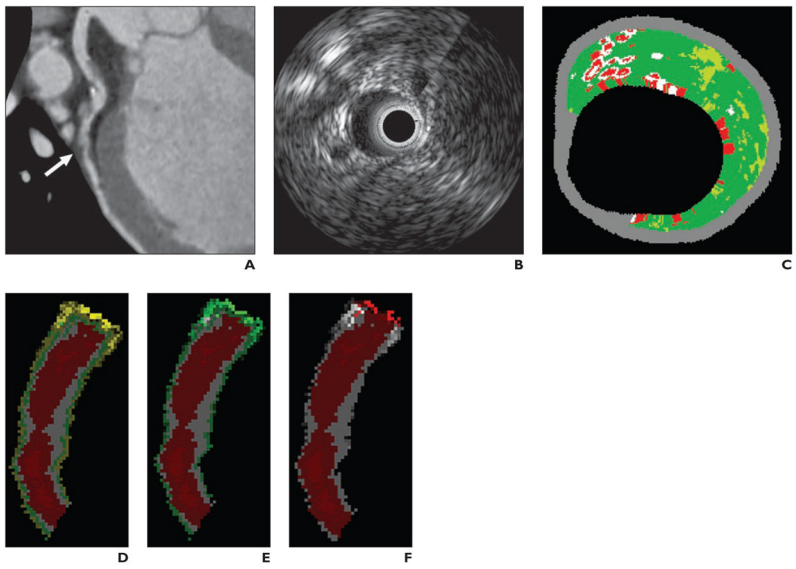

Fig. 3. 61-year-old man with plaque in left anterior descending coronary artery

A, Multiplanar reformation of MDCT angiogram shows noncalcified plaque (*arrow*).

B, Gray-scale intravascular sonogram shows plaque.

C, Intravascular sonographic virtual histologic image shows plaque.

D, Voxel analysis image shows differentiation between lumen (*red*), plaque (*white*), medial layer (*green*), and adventitia (*yellow*).

E, Voxel analysis image with cutoff between adventitia and epicardial fat set at 0 HU with circumferential 0.2-mm voxel subtraction gives plaque plus medial volume.

F, Voxel analysis image shows that subtraction of another voxel is needed to eliminate medial layer and arrive at actual plaque volume on which **C** is based.

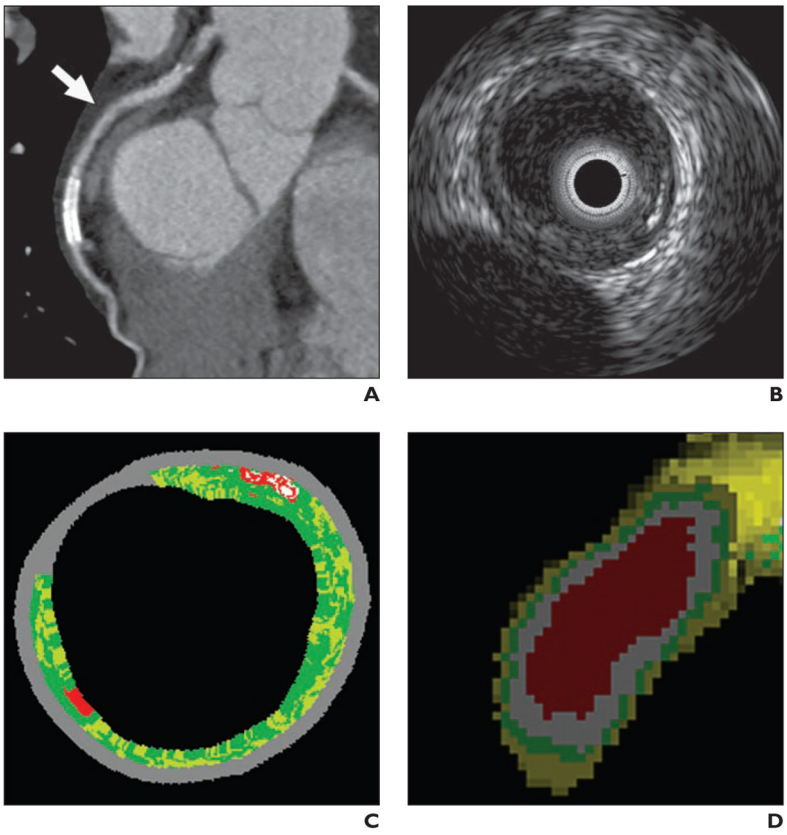

Fig. 4. 66-year-old man with plaque in left anterior descending coronary artery

A, Multiplanar reformation of MDCT angiogram shows discrete circular plaque (*arrow*) in proximal left anterior descending coronary artery.

B, Gray-scale intravascular sonographic image shows plaque.

C, Intravascular sonographic virtual histologic image shows plaque.

D, Voxel analysis image shows segmentation of lumen (*red*), plaque (*white*), medial layer (*green*), and adventitia (*yellow*).